Molecular Crystals and Liquid Crystals

ISSN: 1542-1406 (Print) 1563-5287 (Online) Journal homepage: http://www.tandfonline.com/loi/gmcl20

DSM1-DSM2 Transition Threshold in Turbulent Nematic Mixtures

G. Pucci, F. Carbone, C. Vena, G. Lombardo, C. Versace & R. Barberi

To cite this article: G. Pucci, F. Carbone, C. Vena, G. Lombardo, C. Versace & R. Barberi (2015) DSM1-DSM2 Transition Threshold in Turbulent Nematic Mixtures, Molecular Crystals and Liquid Crystals, 614:1, 100-105, DOI: 10.1080/15421406.2015.1050281

To link to this article: http://dx.doi.org/10.1080/15421406.2015.1050281

Published online: 18 Aug 2015.

Mol. Cryst. Liq. Cryst., Vol. 614: pp. 100–105, 2015

ISSN: 1542-1406 print/1563-5287 online
DOI: 10.1080/15421406.2015.1050281

DSM1-DSM2 Transition Threshold in Turbulent Nematic Mixtures

G. PUCCI,[1,*] F. CARBONE,[2] C. VENA,[1] G. LOMBARDO,[2]
C. VERSACE,[1] AND R. BARBERI[1,2]

[1]Dipartimento di Fisica, Università della Calabria, Rende, Italy
[2]CNR-IPCF UOS of Cosenza, c/o Università della Calabria, Rende, Italy

When forced by a suitable electric field, calamitic nematics can undergo electro-hydrodynamic instabilities and become turbulent. In contrast to isotropic fluid, they present a transition at high forcing from a turbulent regime (DSM1) to a regime characterized by high density of topological defects (DSM2). We study the transition threshold in nematic mixtures with some percent of 5 CB in MBBA. The threshold decreases by increasing the 5 CB concentration, an opposite behavior to what is expected by the increase of dielectric anisotropy. We suggest that the threshold control parameter is the biaxial coherence length, that is of the order of defect size.

Keywords nematics; electro-hydrodynamic turbulence; DSM1-DSM2 transition; biaxial order; biaxial coherence length

1. Introduction

A thermotropic liquid crystal in the nematic phase is usually composed of calamitic molecules made of a flat rigid core and flexible side chains at extremities. The mesophase anisotropy is given by the core, while chains contribute to the stability of the molecular order. Calamitic molecules are often represented as rods with cylindrical symmetry whose average shape is mainly given by fast thermal rotation around the main axis. Most of the electro-optical behaviors of nematics are described in terms of uniaxial order, by considering the dimensionless unit vector n (director) and the uniaxial order parameter $S = \frac{3cos^2\theta - 1}{2}$, where brackets indicate an average over the orientational distribution function of molecules around n and θ is the angle between the molecular axis and the director. S is usually considered constant in space and time and independent by $\boldsymbol{n}$ [1].

The route to turbulence of the electro-hydrodynamics of nematics has been extensively investigated for the common liquid crystal MBBA [2, 3]. Experiments are usually performed using large aspect ratio and transparent cells to confine a nematic layer of thickness some tens of micrometers. The sample is illuminated by polarized light and an optical microscope collects the light it transmits. Starting from an initial planar alignment, the MBBA is forced by a low-frequency (∼100 Hz) oscillating voltage which results in an electric field

*Address correspondence to G. Pucci, Dipartimento di Fisica, Università della Calabria, 87036 Rende, Italy. E-mail: giuseppe.pucci@fis.unical.it

Color versions of one or more of the figures in the article can be found online at www.tandfonline.com/gmcl.

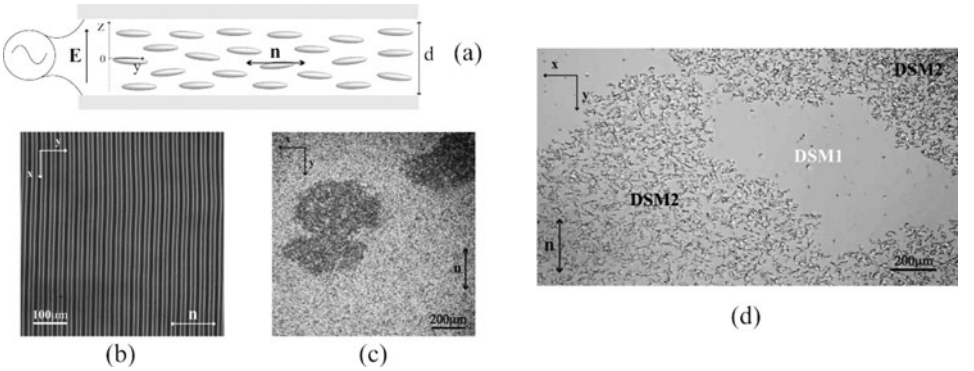

Figure 1. Electro-hydrodynamics of MBBA observed with a polarizing microscope collecting the light transmitted through a sample cell of thickness $d = 24$ μm at forcing frequency $f = 70$ Hz. (a) Schematic representation (out of scale) of a cell filled with nematic in planar alignment $\boldsymbol{n} = (0, 1, 0)$. The voltage $V(t) = \sqrt{2}V_0 cos(2\pi \boldsymbol{f} t)$ is applied, resulting in an electric field $\boldsymbol{E}(z, t) \perp \boldsymbol{n}$. (b) Kapustin-Williams domains observed at the threshold $Vc = 6.4$V. (c) DSM2 nuclei (dark) growing into DSM1 (bright). (d) Snapshot taken 0.1s after the switching off of the voltage during the DSM1-DSM2 transition. Regions in which DSM2 was developed present a much higher density of topological defects.

perpendicular to $\boldsymbol{n}$ [Fig. 1(a)]. Above a first threshold V_C, the system undergoes an electro-convective instability and a periodic modulation of the director is observed. When light polarization is parallel to $\boldsymbol{n}$, this modulation appears as parallel black and white stripes, because of its focusing effect on the incident polarized light [1] [Fig. 1(b)]. These stripes are known as Kapustin-Williams domains [4, 5].

For a slight amplitude step δV above V_C the system is driven out of equilibrium. As the field amplitude increases, the system undergoes a sequence of bifurcations with spatiotemporal states characterized by increasing disorder. The time and space scales decrease continuously until it reaches a turbulent state with the formation of small-scale structures. In this regime, the sample is characterized by patterns on all spatial scales [6, 7]. For higher forcing amplitude, the system reaches the regime known as Dynamic Scattering Mode (DSM1), that strongly scatters the light. Above a second threshold V_T dark regions nucleates into the DSM1. This is another regime known as Dynamic Scattering Mode 2 (DSM2), that expands covering the whole sample [8] [Fig. 1(c)]. The contrast between the two regimes is enhanced by illuminating the sample with light polarized perpendicularly to the initial director alignment. This "filters" the distortions residual from Kapustin-Williams domains present in DSM1. We show the main difference between DSM1 and DSM2 by switching-off the voltage before the DSM2 has covered the whole cell, and taking a picture after t = 0.1 s. Regions in which DSM2 was growing present a high density of disclinations, that are almost absent in regions in which DSM1 was present [Fig. 1(d)]. Inside DSM2 nuclei disclinations are continuously generated, so that the main difference between the two regimes resides in their density, which is much higher in DSM2 than in DSM1 [2, 3].

Disclinations are a type of topological defects, whose core is surrounded by a biaxial ring [9]. Biaxial order usually appears when the frustration constrict the rotational disorder [10] and requires a description in terms of the tensor order parameter $\boldsymbol{Q}$, which couples S and $\boldsymbol{n}$ [11]. Inside the defect core the tensor $\boldsymbol{Q}$ undergoes an eigenvalue exchange through breaking of degeneracy [9]. The scale over which biaxial order extends in a uniaxial medium

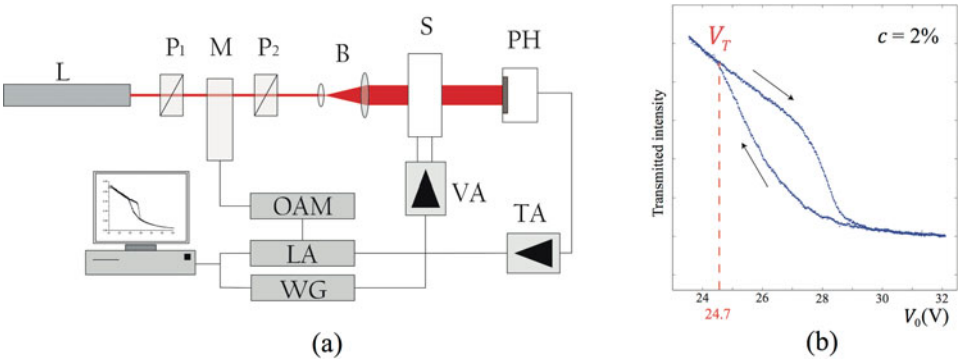

Figure 2. (a) Setup for DSM1-DSM2 threshold measurements. He-Ne laser (L), linear polarizers (P_1, P_2), opto-acoustic modulator (M), beam-expander (B), sample (S), large area photodiode (PH), trans-impedance amplifier (TA), Lock-in amplifier (LA), waveform generator (WG), voltage amplifier (VA). (b) Example of threshold measurement based on the transmitted light intensity. Cell thickness $d = 24\ \mu$m, forcing frequency $f = 70$ Hz, $T = 26.0^{\circ}$C.

is known as *biaxial coherence length* and denoted by ξ_b [12]. A dynamical numerical model has shown that $\xi_b \sim 5$ nm for 5 CB close to the nematic-isotropic transition [13] and recent measurements in the π-cell have given $\xi_b \sim 30$ nm for 5 CB at T = 25°C [14]. These experimental values are presumably overestimated because of the simplified optical model adopted to extrapolate ξ_b, therefore at present the best value for ξ_b is in the order of 5–10 nm. Numerical simulations and related experiments with a π-cell showed that it is possible to control ξ_b with suitable doping of 5 CB with MBBA [15].

In this article, we investigate the DSM1-DSM2 transition threshold in nematic mixtures constituted of some percent of 5 CB in MBBA. We compare this result with complementary measurements of threshold in MBBA samples at different temperatures, where macroscopic quantities as the dielectric anisotropy are expected to change significantly.

2. Experimental Cells

We use two well-known liquid crystals that are in the nematic phase at room temperature, and whose physical properties can be easily found in literature: MBBA (N-(4-Methoxybenzylidene)-4-butylaniline) and 5 CB (4-cyano-4′-pentylbiphenyl). MBBA has negative dielectric anisotropy $\varepsilon_a = -0.53$ [16] and 5 CB has positive dielectric anisotropy $\varepsilon_a = 11.5$ [17] at $T = 25^{\circ}$C. We work with samples of area $A = 1$ cm^2 confined in transparent cells of micrometric thickness $d = 24\ \mu$m. Cells are composed of two parallel glass plates whose inner surfaces are coated by conductive ITO (indium tin oxide) and having the function of electrodes. The inner surfaces are treated in order to impose a strong planar alignment of nematic molecules and the plates are oriented to generate a uniform planar texture in the bulk, corresponding to $\boldsymbol{n} = (0, 1, 0)$ in the quiescent case [Fig. 1(a)].

The voltage $V(t) = \sqrt{2}V_0 cos(2\pi f t)$ is applied across the sample, with fixed frequency $f = 70$ Hz. As a result, an electric field $\boldsymbol{E}(z, t)$ perpendicular to the electrodes is generated. Observations are performed by means of an optical polarizing microscope connected to a CCD camera, which collects the light transmitted through the cell.

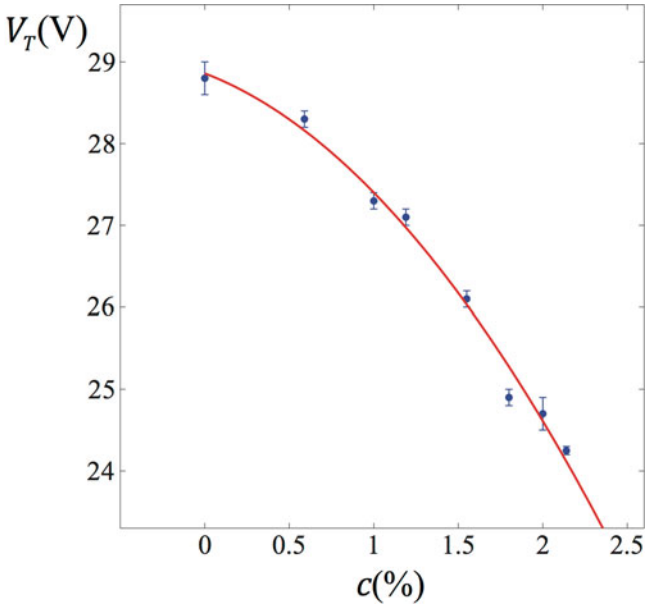

Figure 3. DSM1-DSM2 transition threshold V_T as a function of the weight concentration c of 5 CB in MBBA. The line is a guide for the eyes. Cell thickness $d = 24$ μm, forcing frequency $f = 70$ Hz, $T = 26.0°$C.

3. Setup for Measuring the DSM1-DSM2 Transition Threshold

Threshold measurements are performed by monitoring the light intensity transmitted through the cell during the transition. The temperature of the sample is controlled by means of a double-oven, in which the outer gap is maintained at a lower temperature by a liquid circulation thermostat, while the inner core containing the sample is heated using an alumel wire fed by a DC current regulated power supply. By this method, temperature in the inner core is measured with error in the order of 0.1°C.

The DSM1-DSM2 transition voltage is determined with a method similar to that used by Kai & Zimmermann in their pioneer work on the DSM1-DSM2 transition [8]. The setup is depicted in Fig. 2(a). The cell is illuminated by a linearly polarized beam, whose polarization is oriented perpendicularly to $\boldsymbol{n} = (0, 1, 0)$ to enhance the contrast of DSM2 nuclei in the DSM1 background. The light beam produced by a He-Ne laser is enlarged by a beam-expander to cover the whole surface of the cell electrodes. The intensity of the light beam transmitted by the sample is revealed by a Hamamatsu large area ($\sim$1 cm^2) silicon photodiode. By this method, the measurement is averaged over the whole sample experiencing the electric field. The applied voltage is increased at the rate $r = 4$ m V/s above threshold, then decreased. For each value of voltage, a value of the transmitted light intensity is measured. A forward and a backward curve depicting the transmitted light intensity as a function of the applied voltage are obtained, and their crossing gives the transition threshold [Fig. 2(b)].

4. DSM1-DSM2 Transition Threshold in Nematic Mixtures

We prepare eight different mixtures constituted of 5 CB in the range of weight concentration $c = 0 - 2.5\%$ in MBBA. The dielectric anisotropy of such mixtures is negative and increases

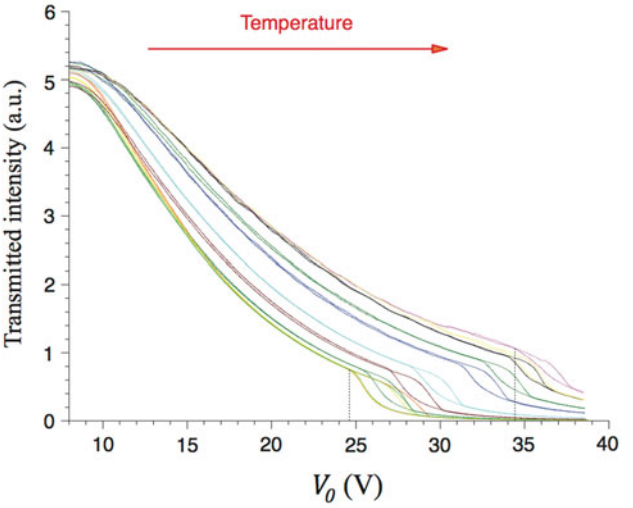

Figure 4. Measurements of the transmitted intensity at the DSM1-DSM2 transition threshold at different temperature. The lowest threshold is $V_T = 24.6$V at $T = 16.0°$C, the highest is $V_T = 34.4$ V at $T = 31.0°$C. Cell thickness $d = 24$ μm, forcing frequency $f = 70$ Hz.

approaching zero at $c = 2.5\%$. With each mixture we fill a cell of thickness $d = 24$ μm, then we measure the DSM1-DSM2 transition threshold for all samples at fixed temperature $T = 26.0°$C. We find that the threshold decreases when c increases [Fig. 3]. One could ascribe this behaviour to the change of dielectric anisotropy from one mixture to another. However, measurements on a MBBA sample at different temperatures invalidate this hypothesis. We present these measurements in the next section.

5. DSM1-DSM2 Transition Threshold in MBBA as a Function of Temperature

In order to check the influence of dielectric anisotropy, we measure the DSM1-DSM2 transition threshold in a MBBA sample at different temperatures [Fig. 4]. The nematic-isotropic transition temperature of the MBBA used is $T_c = 37.5°$C. Being the dielectric anisotropy an indicator of the nematic order, its absolute value decreases approaching the clearing point. Correspondingly, the DSM1-DSM2 threshold increases, as reported in Fig. 4. The absolute value of the dielectric anisotropy decreases also by mixing the MBBA with a small quantity of 5 CB, but there the behaviour is opposite, i.e. the threshold decreases.

6. Conclusion

We investigated the DSM1-DSM2 transition threshold of turbulent nematics in two situations. In the first one, we found that the threshold decreases for nematic mixtures of increasing concentration of 5 CB in MBBA. In the second, we measured that the threshold in sole MBBA samples increases with the temperature. These opposite behaviours suggest that the threshold in the two situations is controlled by different factors. As the dielectric anisotropy variation cannot explain the threshold behavior in the case of MBBA mixed with 5 CB, we should look for another control parameter. We consider the nematic biaxial

coherence length ξ_b, that has already been found to play a relevant role in 5 CB/MBBA mixtures [15]. We notice that the decrease of the DSM1-DSM2 transition threshold in MBBA mixed with 5 CB has an analogue in the π-cell, where the electric field threshold of order reconstruction decreases if ξ_b increases [15]. In both cases, the increase of biaxiality of the system is accompanied by a decrease of the voltage required for the transition, as a larger ξ_b favors biaxial order inside the uniaxial nematic.

In a very simplified picture, 5 CB and MBBA molecules in the presence of an external electric field tend to orient perpendicular to each other because their dielectric anisotropy have opposite sign. As a consequence, when a strong electric field is applied and the nematic field is weak, local biaxial order is favored in the mixture with respect to a single material. In this picture, mixing MBBA with some percent of 5 CB corresponds to increase its biaxial coherence length and hence to reduce the DSM1-DSM2 transition threshold, even if the absolute value of the dielectric anisotropy decreases. Being the DSM1 a turbulent regime, small scale structures are generated and they could be responsible for high stresses at scales in the order of the biaxial coherence length, leading to the high density of disclinations found in DSM2.

Acknowledgments

We are grateful to A. Pane for technical assistance. Università Italo-Francese (UIF) supported this work.

References

[1] P.G. De Gennes, & J. Prost, (1993). *The Physics of Liquid Crystals* Oxford Science Publications.
[2] A. Joets, & R. Ribotta, (1989). *J. Phys. 47*, 595.
[3] S. Kai, & W. Zimmermann, (1989). *Prog. Th. Phys. Supp. 99*, 458.
[4] G.E. Zvereva, & A. P. Kapustin. (1961). In book: *Primenenie ultra-akustiki kissledovaniyu veshchestva (*The *application of ultra-acoustics to the investigation of matter)*, issue 15, Moscow, p. 69 (in Russ.).
[5] R. Williams, (1963). *J. Chem. Phys. 39*, 384.
[6] F. Carbone, L. Sorriso-Valvo, C. Versace, G. Strangi, & R. Bartolino, (2011). *Phys. Rev. Lett. 106*, 114502.
[7] F. Carbone, H. Yoshida, S. Suzuki, A. Fujii, G. Strangi, C. Versace, & M. Ozaki, (2010). *Eur. Phys. Lett. 89*, 46004.
[8] S. Kai, W. Zimmermann, M. Andohand, & N. Chizumi, (1990). *Phys. Rev. Lett. 64*, 1111–1114.
[9] N. Schopol, & T. J. Sluckin, (1987). *Phys. Rev. Lett. 59*, 2582.
[10] M.J. Freiser, (1970). *Phys. Rev. Lett. 24*, 1041.
[11] P.G. de Gennes, (1969). *Phys. Lett. 30A*, 454.
[12] F. Bisi, E. C. Gartland, R. Rosso, & E. G. Virga, (2003). *Phys. Rev. E 68*, 021707.
[13] G. Lombardo, H. Ayeb, & R. Barberi, (2008). *Phys. Rev. E 77*, 051708.
[14] R. Hamdi, G. Lombardo, M. P. De Santo, & R. Barberi, (2013). *Eur. Phys. J. E 36*, 115.
[15] F. Ciuchi, H. Ayeb, G. Lombardo, R. Barberi, & G. E. Durand, (2007). *App. Phys. Lett. 91*, 244104.
[16] A. Hertrich, A. P. Krekhov, & O. A. Scaldin, (1994). *J. Phys. II 4*, 239–252.
[17] B.A. Belyaev, N. A. Drokin, V. F. Shabanov, & V. N. Shepov, (2000). *Phys. Solid State 42*, 577–579.